Developmental Biology **215,** 358–374 (1999)
Article ID dbio.1999.9477, available online at http://www.idealibrary.com on IDEAL®

Engineered Truncations in the Drosophila Mastermind Protein Disrupt Notch Pathway Function

Whitney Helms,* Hyung Lee,* Matthew Ammerman,* Annette L. Parks,† Marc A. T. Muskavitch,† and Barry Yedvobnick*,[1]

**Department of Biology, Emory University, Atlanta, Georgia 30322; and †Program in Genetics, Cell and Developmental Biology, Department of Biology, Indiana University, Bloomington, Indiana 47405*

The phenotypes and genetic interactions associated with mutations in the *Drosophila mastermind* (*mam*) gene have implicated it as a component of the Notch signaling pathway. However, its function and site of action within many tissues requiring Notch signaling have not been thoroughly investigated. To address these questions, we have constructed truncated versions of the Mam protein that elicit dominant phenotypes when expressed in imaginal tissues under GAL4-UAS regulation. By several criteria, these effects appear to phenocopy loss of function for the Notch pathway. When expressed in the notum, truncated Mam results in failure of lateral inhibition within proneural clusters and perturbations in cell fate specification within the sensory organ precursor cell lineage. Expression in the wing is associated with vein thickening and margin defects, including nicking and bristle loss. The truncation-associated wing margin phenotypes are modified by mutations in Notch and Wg pathway genes and are correlated with depressed expression of *wg, cut,* and *vg*. These data support the idea that Mam truncations have lost key effector domains and therefore behave as dominant-negative proteins. Coexpression of Delta or an activated form of Notch suppresses the effects of the Mam truncation, suggesting that Mam can function upstream of ligand–receptor interaction in the Notch pathway. This system should prove useful for the investigation of the role of Mam within the Notch pathway.

Key Words: **Mastermind; Notch pathway; *Drosophila;* wing margin; notum.**

INTRODUCTION

Cell communication and signal transduction are essential developmental processes, and a wide variety of such systems has been described in many organisms (Greenwald and Rubin, 1992). The Notch pathway is one of the more recently characterized signal transduction systems. The pathway comprises a membrane receptor, ligands, and several cytoplasmic and nuclear proteins that are involved in the regulation of target gene expression. Originally described in *Drosophila,* some of the pathway-encoding genes, called the neurogenic loci, were initially associated with lateral inhibition during nervous system formation (Lehmann *et al.,* 1983). These loci were subsequently shown to function in a wide spectrum of tissues throughout *Drosophila* development (Dietrich and Campos-Ortega, 1984; Xu *et al.,* 1990; Corbin *et al.,* 1991; Ruohola *et al.,* 1991; Hartenstein *et al.,* 1992; Bender *et al.,* 1993; Parody and Muskavitch, 1993) and to be evolutionarily-conserved (Artavanis-Tsakonas *et al.,* 1995; Weinmaster, 1997). Components of the Notch pathway have been described in *Caenorhabditis elegans* and numerous vertebrates, including humans, demonstrating fundamental roles in normal development as well as disease processes (Gridley, 1997). The best-described components of the pathway include the Notch receptor, its ligands Delta (Dl) and Serrate (Ser), a cytoplasmic protein Deltex (Dx), the negative regulator Hairless (H), and the nuclear proteins Suppressor of Hairless [Su(H)], Mastermind (Mam), and members of the Enhancer of Split [E(spl)] class of transcription factors (Artavanis-Tsakonas *et al.,* 1995). E(spl) proteins are positively regulated by Notch/Su(H) (Jennings *et al.,* 1994; Bailey and Posakony, 1995; Lecourtois and Schweisguth, 1995) and, in

[1] To whom correspondence should be addressed. Fax: (404) 727-2880. E-mail: Biolby@Biology.Emory.Edu.

0012-1606/99 $30.00

combination with Groucho (Gro), repress target genes (Oellers *et al.*, 1994; Paroush *et al.*, 1994). Repression of genes normally associated with specific pathways of differentiation, such as proneural genes during neurogenesis, is consistent with the suggestion that the Notch pathway can maintain cells in an uncommitted state (Coffman *et al.*, 1993).

The Notch pathway has been studied in several imaginal tissues. In the eye, it is required for numerous cell fate decisions affecting photoreceptors, cone cells, pigment cells, and bristles (Cagan and Ready, 1989; Parks *et al.*, 1995; Baker and Yu, 1997). In the notum, the pathway mediates selection of sensory organ precursor (SOP) cells from proneural clusters and subsequent determination of their progeny (Hartenstein and Posakony, 1990; Parks and Muskavitch, 1993; Bang *et al.*, 1995; Lyman and Yedvobnick, 1995). In the wing, it is critical for vein morphogenesis (de Celis, 1997, Huppert *et al.*, 1997) and establishment of the "D/V" organizer at the junction between the dorsal and the ventral wing compartments (Rulifson and Blair, 1995; Neumann and Cohen, 1996; Kim *et al.*, 1996; de Celis and Bray, 1997; Micchelli *et al.*, 1997; Fleming *et al.*, 1997). During wing patterning, the expression of Notch and its ligands is subject to feedback regulation that produces an asymmetric distribution of these proteins in adjacent cell populations and the subsequent restriction of signaling and reception (de Celis and Bray, 1997; Huppert *et al.*, 1997; Micchelli *et al.*, 1997). At the D/V organizer, Notch activity positively regulates genes that are involved in growth and differentiation, such as *wingless* (*wg*), *vestigial* (*vg*), and *cut* (Rulifson and Blair, 1995; Neumann and Cohen, 1996; Kim *et al.*, 1996; Micchelli *et al.*, 1997; de Celis and Bray, 1997). These genes also require Su(H) function for expression (Neumann and Cohen, 1996). Thus, the Notch pathway regulates the expression of a diverse group of genes and mediates both lateral-inhibitory and inductive events. These processes involve additional genes that may contribute in either a general or a tissue-specific manner to pathway function. For example, not all effects are mediated by Su(H) (Lecourtois and Schweisguth, 1995; Matsuno *et al.*, 1997), and loci such as *strawberry notch* (*sno*) exhibit more limited mutant phenotypes (Majumdar *et al.*, 1997). Furthermore, genetic screens have identified additional pathway components in *Drosophila* (Verheyen *et al.*, 1996; Rooke *et al.*, 1996) and *C. elegans* (Levitan and Greenwald, 1995; Hubbard *et al.*, 1996). Interactions with other signaling systems, such as the Wg, Sevenless (Sev), and epidermal growth factor receptor pathways, have also led to the characterization of genes that affect Notch signaling (Axelrod *et al.*, 1996; Karim *et al.*, 1996; Price *et al.*, 1997). Thus, a major goal in the study of the Notch pathway is to identify and determine the role of each of its components and to understand the basis for cross-communication with other pathways. An analysis of the *Drosophila mastermind* (*mam*) gene is central to this goal.

One of the more enigmatic components of the Notch pathway, *mam* is a member of the original group of zygotic neurogenic loci (Lehmann *et al.*, 1983; Yedvobnick *et al.*, 1988). The *mam* gene is widely expressed and functions throughout *Drosophila* development (Dietrich and Campos-Ortega, 1984; Hartenstein and Campos-Ortega, 1986; Smoller *et al.*, 1990; Bettler *et al.*, 1991; Hartenstein *et al.*, 1992; Schmid *et al.*, 1996; Bettler *et al.*, 1996). The Mam protein comprises a novel sequence with features suggestive of a role in transcriptional regulation, including basic and acidic charge clusters that might mediate interactions with DNA and protein, respectively (Smoller *et al.*, 1990). Consistent with a regulatory role, the protein associates with specific chromosome sites *in vivo* and is often coincident with RNA polymerase II (Bettler *et al.*, 1996). Mutations in *mam* exhibit genetic interactions with *N* (Brand and Campos-Ortega, 1990; Xu *et al.*, 1990), *dx (*Xu and Artavanis-Tsakonas, 1990), and *Su(H)* mutations (Fortini and Artavanis-Tsakonas, 1994). These interactions are evident during wing morphogenesis as the wing phenotypes of *N*, *dx*, and *Su(H)* alleles are enhanced by loss-of-function *mam* mutations. Because *N*, *dx*, and *Su(H)* each encode a key component of the signaling cascade, the genetic interactions imply an important and proximate role for Mam. However, despite the genetic and molecular information available on Mam, its function and site of action within the pathway during critical developmental events have not been thoroughly investigated. To address these questions, we have created transgenic strains expressing mutated Mam proteins that effectively depress *mam* function in a stage and tissue-specific manner. This was accomplished by engineering truncated versions of Mam that were placed under *GAL4-UAS* regulation (Brand and Perrimon, 1993). Using this system, we show that Mam truncations elicit imaginal phenotypes consistent with those associated with loss-of-function mutations in other Notch pathway loci. In the wing, these phenotypes are modified by mutations in Notch and Wg pathway genes and are correlated with depressed expression of the Notch pathway target genes *cut*, *vg*, and *wg*. The highly penetrant dominant phenotypes produced by this system facilitated epistasis studies to position Mam action within the Notch pathway. The results of these studies support the idea that Mam can function in the Notch pathway upstream of ligand–receptor interaction during wing margin formation.

MATERIALS AND METHODS

Drosophila Strains

GAL4 driver strains. *C96-GAL4* drives at the wing margin (Gustafson and Boulianne, 1996). *sevhs-GAL4* drives in sets of cells posterior to the eye furrow (Fortini *et al.*, 1993), and *309-GAL4* drives in proneural clusters of the wing disc (Artavanis-Tsakonas, personal communication). *glass-GAL4* drives in cells posterior to the eye furrow (Freeman, 1996). *blk-GAL4* drives along the anterior/posterior wing boundary and in the leg and eye disc (Morimura *et al.*, 1996). *pnr-GAL4* drives from the future notal midline to prospective microchaete stripe 5 (Heitzler *et al.*, 1996a).

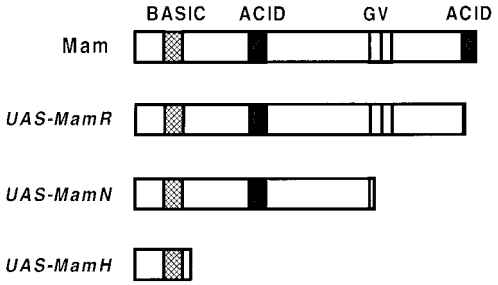

FIG. 1. Mam truncation constructs cloned into pUAST. The top diagram (Mam) shows the general structure of the full-length Mam protein, containing three charged amino acid clusters and three runs of alternating glycine and valine (GV). Additional features of the protein sequence are described in Smoller *et al.* (1990) and Bettler *et al.* (1996). UAS-MamR eliminates a small carboxy-terminal segment of the protein that includes most of the second acidic cluster. UAS-MamN removes sequences located carboxy to the first GV region, and UAS-MamH removes sequences carboxy to the basic cluster. Details of the constructions are given under Materials and Methods.

UAS strains. The *UAS* strains used were Dl, *UAS-DlWT1;* Ser, *UAS-SerD;* N, *UAS-N^{actW};* Dx, *UAS-DxA89;* Su(H), *UAS-Su(H)/Cy;* H, *UAS-H3;* Dfz2, *UAS-Dfz263-10;* Dsh, *UAS-Dsh3;* Zw3, *UAS-Zw310a;* Arm, *UAS-Arm^{S2A}* and *UAS-Arm^{S10C};* and dTCF, *UAS-dTCF10.*

Other strains. The other strains used were *w^{1118}; H^{1} Pr/In(3R)C e, arm^{1}/FM7c, (dTCF) pan^{13a}/ey^{D}, P{ry^{+}t7.2 = neoFRT}43D P{w^{+}mC = πM}46F P{w^{+}mC = πM}47F FRT43-2πM, wg^{CX4}/CyO, zw3^{M11-1}/FM7, dsh^{v26}/FM7, y w^{a} N^{5419}; C(1)DX ywf; Dp(1;2)w^{+51b7}, nd^{1}, ec dx^{1}, st e E(spl)^{8D06}/TM3, gro^{E48}/TM6B, mam^{N2G}/Cy, ss Dl^{BX9} e^{4} ro/TM6C, e Bd^{G}/TM6B, red Ser^{rev6-1}/TM3, Su(H)^{S5}/CyO, Su(H)^{SF8} Adh^{up3} cn/CyO, vg-LacZ, w; P[FRT]43D mam^{IL115}/CyO, w hsFLP; Sco/Cy, cm cut^{53d}.*

Strain descriptions can be found in Lindsley and Zimm (1992) and Flybase. All crosses were performed at 25°C.

Construction of UAS-Mam Truncations

Subclones of the 6333-nucleotide Mam cDNA B4 (Smoller *et al.*, 1990) in pUAST (Brand and Perrimon, 1993) were created as follows. The constructs are diagrammed in Fig. 1. The full-length Mam open reading frame (ORF) predicts a protein of 1596 residues. For UAS-MamR, which terminates at nucleotide 5446, B4 was cut with *Eco*RI and a 5.7-kb fragment was cloned into pUAST. This fragment of Mam contains the entire ORF except for the carboxy-terminal 32 residues, which contain the majority of sequence within the second acidic charge cluster. For UAS-MamN, which terminates at nucleotide 3884, the UAS-MamR clone was cut with *Not*I at an internal site and also within the pUAST polylinker. The fragment corresponding to UAS-MamN was self-ligated. This construct encodes through the first acidic charge cluster, as well as an additional 500 residues, ending at Mam residue 1043; it eliminates two of three Gly-Val runs. For UAS-MamH, which terminates at nucleotide 1489, cDNA B4 was cut with *Eco*RI and *Hinc*II, and a 1.8-kb fragment was cloned into pBluescript KS (Stratagene) between the *Eco*RI and *Sma*I sites. The MamH segment was excised with *Eco*RI and *Xba*I and cloned into pUAST. This truncation ends at Mam residue 245, 55 residues carboxy to the basic charge cluster. It eliminates both acidic charge clusters and all other sequences carboxy to residue 245. Constructs were transformed into the *w^{1118}* strain using standard techniques (Rubin and Spradling, 1982).

Mounting of Adult Tissues

Wings were dehydrated in isopropanol and mounted in Euparol. For nota and eyes, adults were mounted on slides with adhesive and photographed.

Antibody Staining of Third-Instar Larval Wing Discs

The protocol of Brennan *et al.* (1998) was followed for the fixation, staining, and washing of imaginal discs. Images were obtained using a Bio-Rad MRC 1024 confocal microscope. The following antibodies/dilutions were used: Mam (1:1000 rat polyclonal; Bettler *et al.*, 1996), Wg (1: 20 mouse monoclonal; R. Nusse), β-galactosidase (1: 100 mouse; Promega), Cut (1:20 mouse monoclonal; Developmental Studies Hybridoma Bank), and c-Myc (1:100 rabbit polyclonal, A-14-G; Santa Cruz Biotechnology). FITC and Cy5 secondary antibodies were obtained from Jackson ImmunoResearch Laboratories and used as described previously (Bettler *et al.*, 1996).

Antibody Staining of Pupal Nota

Monoclonal antibody 22C10 (Seymour Benzer) recognizes a cytoplasmic epitope expressed primarily in neuronal cells (Zipursky *et al.*, 1984; Hartenstein, 1988). Monoclonal antibody 990 E5 F1 (Sean Carroll) recognizes the Achaete protein. Goat anti-mouse secondary antibody conjugated to horseradish peroxidase was obtained from Jackson Immunochemicals. Immunolocalization was carried out as described in Parks *et al.* (1997). For Achaete staining, the color reaction was intensified using silver enhancement (Gallyas *et al.*, 1982; Liposits *et al.*, 1984). In some instances, parts of two or more micrographs were combined in a montage to generate a continuous image of the disc epithelium.

Generation of mam Mosaics

w hsFLP; Sco/Cy females carrying an X chromosome source of FLP recombinase were crossed with *w; P[FRT]43D mam^{IL115}/CyO* males. *Cy*, non-*Sco* males were mated to homozygous females containing FRT at 43D and a Myc protein marker (strain described above). Embryos were collected for 8 h, aged an additional 72 h, and then heat-shocked at 37°C for 60 min to induce FLP. When larvae reached late third instar they were heat-shocked to induce Myc expression and then allowed to recover 30 min prior to dissection. After fixation, wing discs were double-stained with anti-Myc and anti-Cut, as described above.

RESULTS

Production of Dominant Phenotypes through GAL4-UAS-Mediated Overexpression of Mam Truncation Products

The predicted amino acid sequence of Mam suggests a function in transcriptional regulation. The sequence contains three clusters of charged amino acids, an amino-

terminal basic cluster, and two acidic clusters, as well as three unusual runs of alternating glycine-valine (Smoller *et al.*, 1990; Fig. 1). The basic region contains a nuclear localization sequence (Robbins *et al.*, 1991) and limited sequence similarity to a subset of bZip DNA-binding domains. Although no sequence-specific DNA-binding activity has been observed for Mam, the protein associates with a discrete set of transcriptionally active sites on polytene chromosomes (Bettler *et al.*, 1996). Given the absence of strong sequence similarity to known proteins, we reasoned that the charge clusters and Gly-Val repeats of Mam might represent important functional domains. The sequence conservation between *Drosophila melanogaster* and *D. virilis* within the charge clusters and a portion of the Gly-Val repeats supports this reasoning (Newfeld *et al.*, 1993). We predicted that truncations of Mam that eliminate acidic charge clusters, and/or Gly-Val repeats, but retain nuclear targeting via the basic region, might be useful for production of dominant phenotypes. In principle, such truncations could compete with wild-type protein and depress Mam function below 50%, a level of activity that is not associated with reproducible dominant phenotypes (B.Y., unpublished observation). This approach was further encouraged by the characterization of a *mam* mutation associated with a dominant wing-nicking phenotype, *In(2R)N2G* (mam^{N2G}). This *mam* allele is predicted to encode a truncated protein that terminates after the basic region (Smoller *et al.*, 1990). The wing-nicking phenotype of mam^{N2G} is not completely penetrant and is very sensitive to genetic background effects. Therefore, truncation constructs were cloned into pUAST (Brand and Perrimon, 1993) to allow *in vivo* expression at high levels.

Strains containing the MamR, MamN, and MamH truncations in pUAST were constructed (Fig. 1). Transformant lines carrying each construct were crossed to *GAL4* lines that drive in imaginal tissues known to express Mam (Schmid *et al.*, 1996; Bettler *et al.*, 1996), including the wing, eye, and notum. Several *GAL4* lines produce adult phenotypes when combined with the *MamN* and *MamH* truncations. A completely penetrant rough eye phenotype is produced in *glass-GAL4/UAS-MamN* and *UAS-MamN/+; sev-GAL4/+* flies (Figs. 2P–2S). We tested *glass-GAL4/UAS-MamN* flies for genetic interactions and did not observe modifications to the eye phenotype by mutation of *mam* or other Notch pathway loci, except for a very weak enhancement by Dl^{BX9} (data not shown). However, strains heterozygous for this *Dl* allele also exhibit minor eye roughness.

Expression of Truncated Mam in the Notum Elicits Phenotypes Similar to Those Associated with Notch Pathway Loss-of-Function Mutations

A bristle, consisting of a shaft, a socket, a neuron, and a thecogen cell, arises from a single SOP cell that is specified within a proneural cluster (Hartenstein and Posakony, 1989). The Notch pathway functions in cellular specification at multiple steps during bristle development (Hartenstein and Posakony, 1990; Parks and Muskavitch, 1993). The *309-GAL4* driver is expressed in proneural clusters of the wing disc (Fig. 2N) and when combined with *UAS-MamN* or *UAS-MamH* produces changes in bristle number. A recombinant chromosome designated *309-MamH* contains both the *309-GAL4* and the *UAS-MamH* transgenes. *309-MamH/+* nota contain additional macrochaetes, most notably at scutellar (Fig. 2C) and posterior notopleural sites (Fig. 2G). These effects are enhanced in flies heterozygous for certain *mam* alleles (Figs. 2D and 2H). Additionally, mutations in other Notch pathway genes variably enhance the *309-MamH/+* bristle phenotype, and heterozygotes for a *N* locus deletion (N^{5419}) exhibit a lethal interaction (data not shown).

In the heminotum, *pnr-GAL4* directs expression from the future notal midline to prospective microchaete stripe 5 (the stripe which contains the dorsocentral macrochaetes). *pnr-GAL4/UAS-MamN* adults exhibit microchaete loss between the dorsocentral macrochaetes; the phenotypic severity ranges from bald nota to those sparsely populated with bristles (Fig. 3A). Similar bald patches are observed in nota containing mosaic clones homozygous for the severe mam^{IL115} allele (Fig. 3A, lower inset). In addition, *pnr-GAL4/UAS-MamN* animals exhibit additional macrochaetes, twin shafts at some microchaete sites, and twin to quadruple shafts at some macrochaete sites (primarily the scutellar macrochaetes, Fig. 3A, upper inset). The absence of microchaetes could be due to loss of precursors during SOP specification or, alternatively, due to transformation of the shaft and socket cells into neuronal cells at the four-cell stage. We examined SOP specification in *pnr-GAL4/UAS-MamN* animals by staining pupal nota at 13 h after puparium formation (APF) with antibodies to Achaete, which is expressed only in SOP cells at this stage (Parks and Muskavitch, 1993). We observe an increase in the number of SOPs in *pnr-GAL4/UAS-MamN* nota (Fig. 3C) compared to control nota (Fig. 3B). Supernumerary SOPs are also seen in animals following reductions in Notch or Delta function (Hartenstein and Posakony, 1990; Parks and Muskavitch, 1993).

We next examined 35-h APF nota from *pnr-GAL4/UAS-MamN* flies with MAb 22C10, which recognizes shaft and neuron cells of the bristle (Hartenstein and Posakony, 1989). Compared to control nota (Fig. 3D), most microchaetes appear to exhibit only neuronal cell staining (Fig. 3E, inset shows higher magnification). Reduction of Notch or Delta function during specification of bristle organ cells results in similar neuronal clusters (Hartenstein and Posakony, 1990; Parks and Muskavitch, 1993). Similarly, the presence of twin shafts at some microchaete sites indicates a transformation at the four-cell stage of socket cell to shaft cell, a phenotype associated with loss of Notch signaling (Schweisguth and Posakony, 1994; A. L. Parks, T. R. Parody, and M. A. T. Muskavitch, unpublished observation).

MAb 22C10 staining also reveals that multishafted macrochaete groups are associated with multiple neurons, sug-

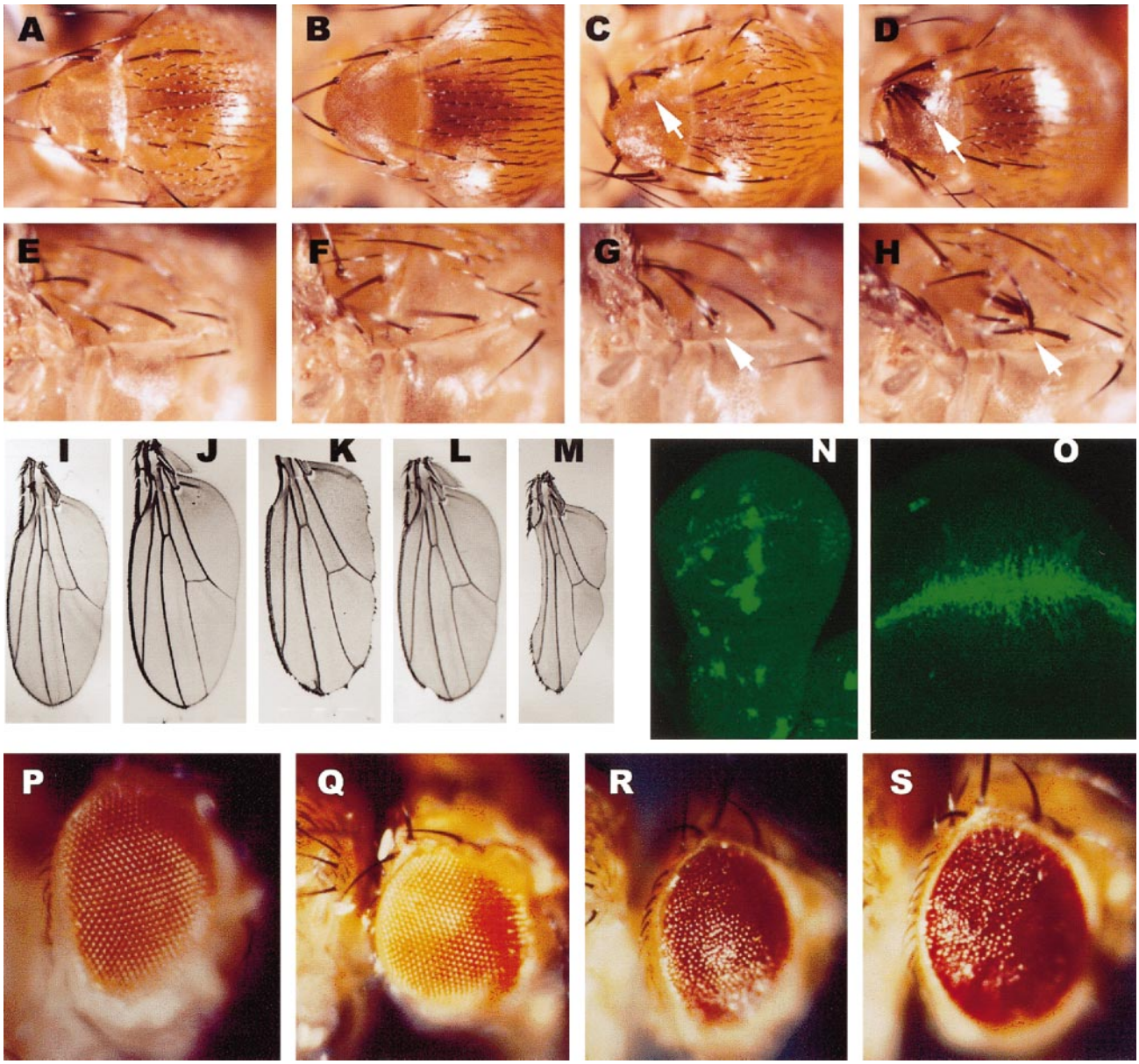

FIG. 2. Imaginal phenotypes associated with overexpression of Mam truncations. Strains containing pUAST Mam constructs were crossed to *GAL4* lines that direct expression in imaginal discs, and the progeny were scored for highly penetrant phenotypes. *UAS-MamR* exhibits only weak effects with certain *GAL4* lines, whereas *UAS-MamN* and *UAS-MamH* produce very strong phenotypes that are in some cases completely penetrant. *309-GAL4* expresses in proneural clusters of the notum (N) and when combined with *UAS-MamH* elicits perturbations in bristle number predominantly at scutellar (A–D) and notopleural (E–H) sites. Control *UAS-MamH*/+ (A and E) and *309-GAL4*/+ (B and F) nota exhibit normal macrochaete number, except for a low frequency of scutellar duplications in *UAS-MamH*. In contrast, nota from recombinant *309-MamH*/+ animals exhibit macrochaete duplications at most scutellar sites and at posterior notopleural sites (C and G, arrows). Nota from mam^{N2G}/*309-MamH* animals show an enhanced macrochaete multiplication phenotype (D and H, arrows). *C96-GAL4* expresses along the wing margin (O) and when combined with *UAS-MamH* produces wing nicks and loss of margin bristles (I–M). Control *C96-GAL4*/+ and *UAS-MamH*/+ wings are normal (I and J, respectively), whereas the heterozygote carrying the recombinant chromosome (*C96-MamH*/+) exhibits wing nicking and bristle loss from anterior and posterior margins and the distal wing tip (K). Wings from a mam^{N2G}/+ heterozygote show a minor nicking phenotype that is incompletely penetrant (L). Wings from mam^{N2G}/+; *C96-MamH*/+ animals exhibit an enhanced phenotype (M) that is also incompletely penetrant. *glass-GAL4* and *sev-GAL4* express in cells posterior to the morphogenetic furrow and when combined with *UAS-MamN* produce rough eyes. Homozygotes for *glass-GAL4* do show minor eye roughness; however, heterozygotes for *glass-GAL4* appear normal under a dissecting scope (P); *sev-GAL4*/+ eyes (data not shown) and *UAS-MamN*/+ eyes (Q) also appear normal. The combinations *glass-GAL4*/*UAS-MamN* (R) and *UAS-MamN*/+; *sev-GAL4*/+ (S) produce a completely penetrant rough eye phenotype. The phenotype associated with a recombinant *glass-MamN* chromosome is not detectably modified by mutations in *mam* or any other Notch pathway gene, except for a slight enhancement by *Dl* (data not shown).

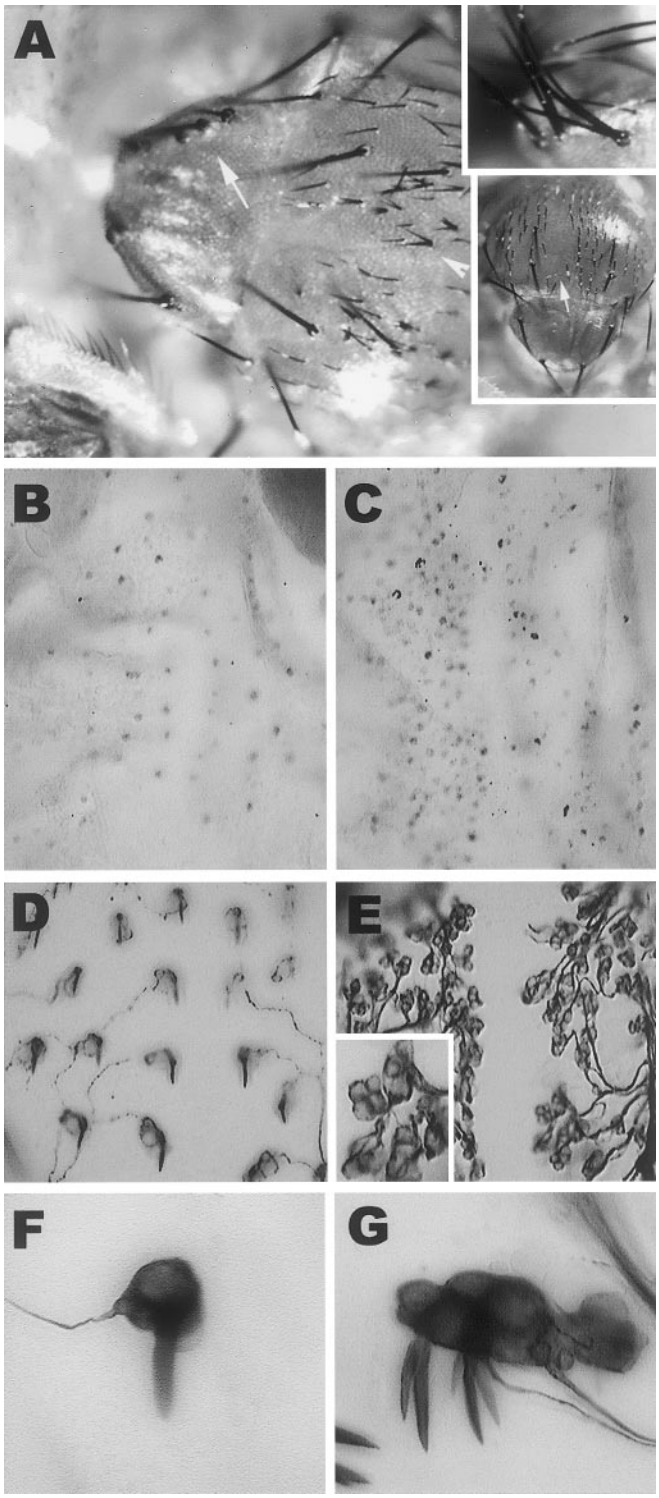

FIG. 3. Mam truncation phenotypes in the notum resemble *N* and *Dl* loss-of-function phenotypes. Adult notum from a *pnr-GAL4/UAS-MamN* fly. (A) Microchaete loss is evident throughout the central region of the notum. In other nota, the central regions are devoid of all microchaetes (bald), and more anterior/lateral regions of the notum contain higher than normal microchaete densities (data not shown). Bald regions are also observed in mam^{IL115}/mam^{IL115} mosaic nota (lower inset, arrow). Supernumerary macrochaetes (arrow) and twin microchaete shafts (arrowhead) are observed in *pnr-GAL4/UAS-MamN* nota. Macrochaete multishafted groups sometimes arise in the scutellar region (upper inset). Achaete staining in a 13-h APF control *A101/TM3* notum reveals a regular array of SOPs (B). Supernumerary SOPs are detected with Achaete antibody in a 13-h *pnr-GAL4/UAS-MamN* notum (C). At 35 h APF, MAb 22C10 stains both the microchaete shaft cells and the neurons in a control *A101/TM3* notum (D). In contrast, MAb 22C10 staining reveals clusters of neurons at each microchaete site in a *pnr-GAL4/UAS-MamN* notum (E). A single neuron and shaft cell are stained by MAb 22C10 at a posterior scutellar macrochaete site in a control *A101/TM3* notum (F). Multiple neurons and several large polyploid cells (shaft and socket cells are both polyploid in bristle organs, and the socket cell will sometimes stain with MAb 22C10) are found at a posterior scutellar macrochaete site in *pnr-GAL4/UAS-MamN* animals (G).

gesting the presence of complete bristle organs and therefore the specification of supernumerary SOPs (Fig. 3G). In some cases, multiple shafts appear to be associated with a single cell body. This phenotype may be similar to multishafted bristles seen in clones of cells carrying deletions of genes within the *E(spl)* complex (Heitzler *et al.*, 1996b) or with reduction of Notch signaling associated with overexpression of *Hairless* (Bang and Posakony, 1992).

Expression of Truncated Mam at the Dorsal/Ventral Wing Boundary Perturbs Wing Margin Formation

Notch pathway function is essential for proper development of the wing margin, therefore we tested the effects of truncated Mam expression on margin formation. The *C96-GAL4* driver is expressed along the dorsal–ventral wing margin (Fig. 2O), as reported previously by Gustafson and Boulianne (1996). Margin nicks and bristle loss are evident in *C96-GAL4/UAS-MamH* wings or wings of *C96-MamH/+* flies (*C96-MamH* is a recombinant chromosome that contains the *C96-GAL4* and *UAS-MamH* transgenes) (Fig. 2K). The wing-nicking phenotype can be enhanced by heterozygosity for mam^{N2G}, although the enhancement is not fully penetrant (Figs. 2L and 2M). Similar wing phenotypes are observed in *C96-GAL4/UAS-MamN* animals (described below); however, only minor wing effects with low penetrance are observed with *C96-GAL4/UAS-MamR* flies (Fig. 4D).

Notch Pathway Mutations Modify the Mam Truncation Wing Phenotype

The phenotype associated with the recombinant *C96-MamN/+* genotype consists of anterior and posterior wing margin loss (nicks) and associated bristle loss (Fig. 4A). In wings from *C96-MamN/+* flies, the most significant mar-

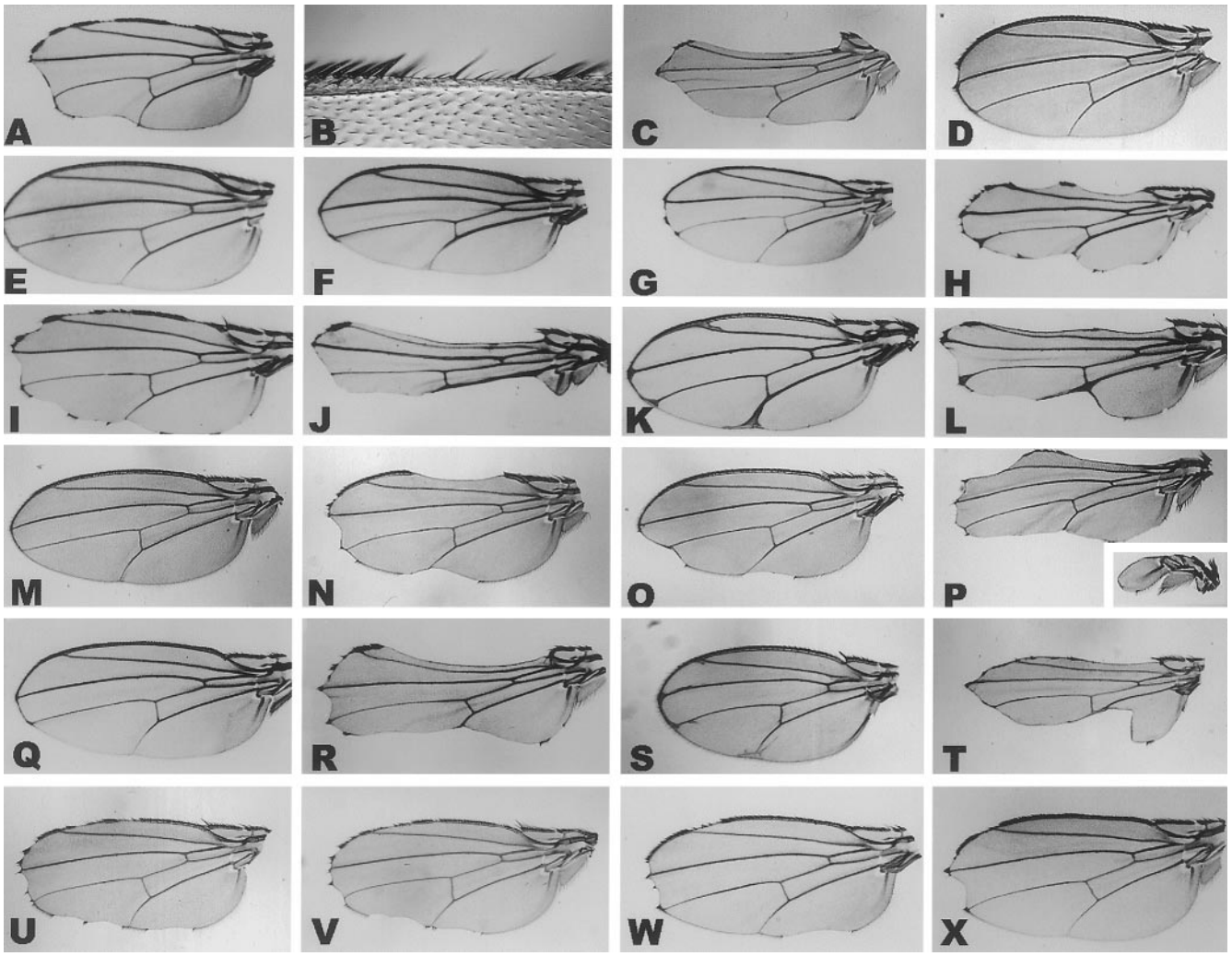

FIG. 4. The *C96-MamN* truncation wing phenotype is modified by mutations of other Notch pathway genes. These studies utilized a recombinant chromosome that contains both the *C96-GAL4* and the *UAS-MamN* transgenes and is referred to as *C96-MamN*. The *C96-MamN*/+ genotype yields a completely penetrant phenotype including nicks and variable bristle loss along the anterior and posterior wing margins (A, B), very similar to the *C96-MamH*/+ phenotype described earlier. The phenotype is significantly more severe in *C96-MamN*/*C96-MamN* homozygotes (C). Expression of *UAS-MamR* under *C96-GAL4* regulation (*C96-GAL4*/*UAS-MamR*) elicits a minor wing-nicking phenotype at low frequency (D). Parental strain w^{1118} (E). *C96-MamN*/*TM3, Sb* flies were crossed with those carrying Notch pathway mutations and scored for modification of the wing phenotype; all controls (except for nd^1/Y *and* dx^1/Y) are heterozygous for w^{1118}. nd^1/Y causes a minor wing-nicking phenotype (G) that strongly enhances the phenotype of *C96-MamN*, as shown for nd^1/Y; *C96-MamN*/+ flies (H). N^{5419}/+ wings show a minor and incompletely penetrant wing phenotype in the w^{1118} genetic background (F). N^{5419}/+; *Dp (1:2)w+51b7*/+; *C96-MamN*/+ flies contain a second chromosome duplication of the wild-type *N* locus and show the typical *C96-MamN* phenotype (I). N^{5419}/+; *C96-MamN*/+ flies do not carry the N^+ duplication and therefore are heterozygous for *N;* they exhibit severely enhanced wings (J). Wings from Dl^{BX9}/+ controls show a typical *Dl* mutant phenotype (K), whereas those from Dl^{BX9}/*C96-MamN* show significantly enhanced wing phenotype (L). Wings from Ser^{rev6-1}/+ are normal (M), whereas those from Ser^{rev6-1}/*C96-MamN* are enhanced (N). Wings from Bd^G/+ show loss of material (O), and those from Bd^G/*C96-MamN* exhibit severely enhanced wing phenotypes (P). The inset in (P) shows the wing phenotype observed in a smaller percentage of cases; the wing blade is nearly absent. The $Su(H)^{S5}$ allele is a gain-of-function mutation (Fortini and Artavanis, 1994). $Su(H)^{S5}$/+ wings are normal (Q), whereas $Su(H)^{S5}$/+; *C96-MamN*/+ wings show an enhanced phenotype (R). Wings from dx^1/Y flies exhibit minor wing perturbations associated with extra vein material (S), whereas those from dx^1/Y; *C96-MamN*/+ flies exhibit significantly enhanced loss of margin and wing blade (T). Wings from flies heterozygous for a deficiency of the *E(spl)* complex, $E(spl)^{8D06}$, or a null mutation in *gro*, gro^{E48}, are normal (data not shown). Wings from $E(spl)^{8D06}$/*C96-MamN* (U) and gro^{E48}/*C96-MamN* (V) do not appear enhanced. *In(3R)C, e*/*C96-MamN* (H^+/H^+) wings exhibit a typical *C96-MamN*/+ wing phenotype (W); this phenotype is partially suppressed by a mutation of the negative Notch pathway regulator *H;* e.g., an H^1/*C96-MamN* wing (X). This genotype produces a range of phenotypes, with some wings rescued more and others less than the wing presented.

gin loss occurs along distal and posterior wing regions. Within some affected regions, the margin is largely intact; however, most bristles, particularly those of the stout mechanosensory class, are missing (Fig. 4B). The *C96-MamN/C96-MamN* phenotype is associated with significant wing blade loss (Fig. 4C).

The *C96-MamN/+* phenotype is enhanced by *N* mutations. Males hemizygous for nd^1 exhibit a minor wing-nicking phenotype (Fig. 4G), and females heterozygous for N^{5419} have a weakly-penetrant wing-nicking phenotype (Fig. 4F). The nd^1*/Y; C96-MamN/+* (Fig. 4H) and N^{5419}*/+; C96-MamN/+* (Fig. 4J) genotypes produce enhanced wing margin effects. N^{5419}*/+;* $Dp(1;2)w^{+51b7}$*/+; C96-MamN/+* females that carry a N^+ duplication on chromosome 2 exhibit a typical Mam truncation phenotype (Fig. 4I). Synergism is also observed with mutations in *Dl* (Figs. 4K and 4L), *Ser* (Figs. 4M–4P), *Su(H)* (Figs. 4Q and 4R), and *dx* (Figs. 4S and 4T). In the case of *Su(H)*, interactions were observed with a gain-of-function allele $Su(H)^{S5}$, but not with loss-of-function alleles, such as $Su(H)^{SF8}$ (data not shown). Deletion of the *E(spl)* complex and point mutations in *groucho* do not enhance the *C96-MamN* phenotype (Figs. 4U and 4V), whereas reduction in the function of *H*, a negative pathway regulator (Maier *et al.*, 1992; Schweisguth and Posakony, 1994), suppresses the phenotype (Figs. 4W and 4X).

Truncated Mam Elicits Loss-of-Function-like Effects and Depresses Expression Levels of Notch Pathway Targets

During wing margin formation, the Notch pathway activates genes involved in patterning, including *cut*, *vg*, and *wg* (Rulifson and Blair, 1995; Neumann and Cohen, 1996; Kim *et al.*, 1996; de Celis and Bray, 1997; Micchelli *et al.*, 1997; Sun and Artavanis-Tsakonas, 1997). When driven at the margin, MamN depresses the expression of Cut (Figs. 5A and 5B), a *vg-LacZ* reporter (Figs. 5C and 5D), and Wg (Figs. 5E and 5F). For Cut, gaps in expression are always evident, whereas for *vg-LacZ* the effects are more variable in severity. The effects on Wg are more uniform and severe than those observed for Cut or *vg-LacZ*. Because the *C96-GAL4* enhancer trap line also expresses at the wing margin, we determined whether MamN affects its expression. *LacZ* expression was assayed in *C96-GAL4/UAS-LacZ* wing discs and *C96-MamN/UAS-LacZ* wing discs. A small, reproducible depression of *C96*-mediated *LacZ* expression was observed in the presence of MamN (Figs. 5G and 5H).

The effects on target gene expression were corroborated by driving MamN along the anterior/posterior (A/P) wing boundary utilizing a *blk-GAL4* construct, which contains the *dpp* 3′ disc enhancer (Morimura *et al.*, 1996). The *blk-GAL4/UAS-MamN* genotype produces phenotypes in the notum, wing, and eye (Figs. 6J–6L), within domains of *dpp* expression in imaginal discs (Masucci *et al.*, 1990). Macrochaete duplications, a deep wing incision, thickening of wing vein 3, and smaller, roughened eyes are observed. The eye phenotype is enhanced by mutations in *mam*, *N*, and *Dl* (Figs. 6M–6O). At the intersection of the A/P and D/V boundaries, expression of Cut (Figs. 6A–6C), *vg-LacZ* (Figs. 6D–6F), and Wg (Figs. 6G–6I) are eliminated by MamN. However, *vg-LacZ* expression persists in a group of MamN-positive cells immediately anterior to the A/P boundary. Additionally, MamN expression within the hinge region does not depress Wg accumulation; similar observations were obtained by others using dominant-negative forms of Delta and Serrate (Sun and Artavanis-Tsakonas, 1997). Thus, overexpression of MamN decreases Notch pathway target gene expression along the wing margin, consistent with its phenotypic effects and genetic interactions.

To determine whether MamN was eliciting an effect similar to *mam* loss-of-function genotypes, mosaic clones of the severe allele mam^{IL115} were produced (Xu and Rubin, 1993). Homozygous *mam* clones were analyzed for expression of Cut; clones that cross the wing margin lose Cut expression (Figs. 5I–5K). Additionally, adults that emerge in these experiments often exhibit wing margin defects (Fig. 5L). These data strongly suggest that the MamN protein acts in a dominant-negative fashion.

The Mam Truncation Wing Phenotype Is Rescued by Overexpression of Delta and an Activated Form of Notch, Suggesting a Role for Mam Upstream of Notch during Margin Formation

The availability of *UAS*-regulated Notch pathway components allowed us to examine their genetic interactions with the *C96-MamN* truncation and investigate their relative order of function within the Notch signaling cascade. If overexpression of another pathway component could rescue the wing phenotype produced by MamN, it would argue for MamN action upstream of that component. Conversely, the inability to rescue the MamN phenotype would favor placement of MamN downstream of that component.

The *C96-MamN* strain was crossed with various *UAS* strains and the wing-nicking phenotypes of the progeny were analyzed. *UAS-Dl* (Figs. 7A and 7B) and an activated form of Notch, $UAS\text{-}N^{actW}$ (Figs. 7E and 7F), strongly suppress the MamN wing-nicking phenotype, implying that the Mam truncation disrupts a function upstream of Delta–Notch interaction. *UAS-Ser* (Figs. 7C and 7D) shows much less rescuing activity. Overexpression of *UAS-H*, a negative pathway regulator of Notch signaling, enhances the wing phenotype (Figs. 7K and 7L). Neither *UAS-Dx* (data not shown) nor *UAS-Su(H)* (Figs. 7I and 7J) rescues the *C96-MamN* phenotype.

C96-GAL4-mediated overexpression of *UAS-Dl*, *UAS-Ser*, $UAS\text{-}N^{actW}$, or *UAS-Su(H)* elicits effects on margin bristle formation, including gain and loss of bristles, as well as formation of double sockets. Wings from $UAS\text{-}N^{actW}$*; C96-GAL4/+* flies exhibit loss of bristles and formation of double sockets, gain-of-function Notch phenotypes (Lyman and Yedvobnick, 1995) (Fig. 7G). *C96-MamN* does not suppress this phenotype (Fig. 7H), consistent with MamN

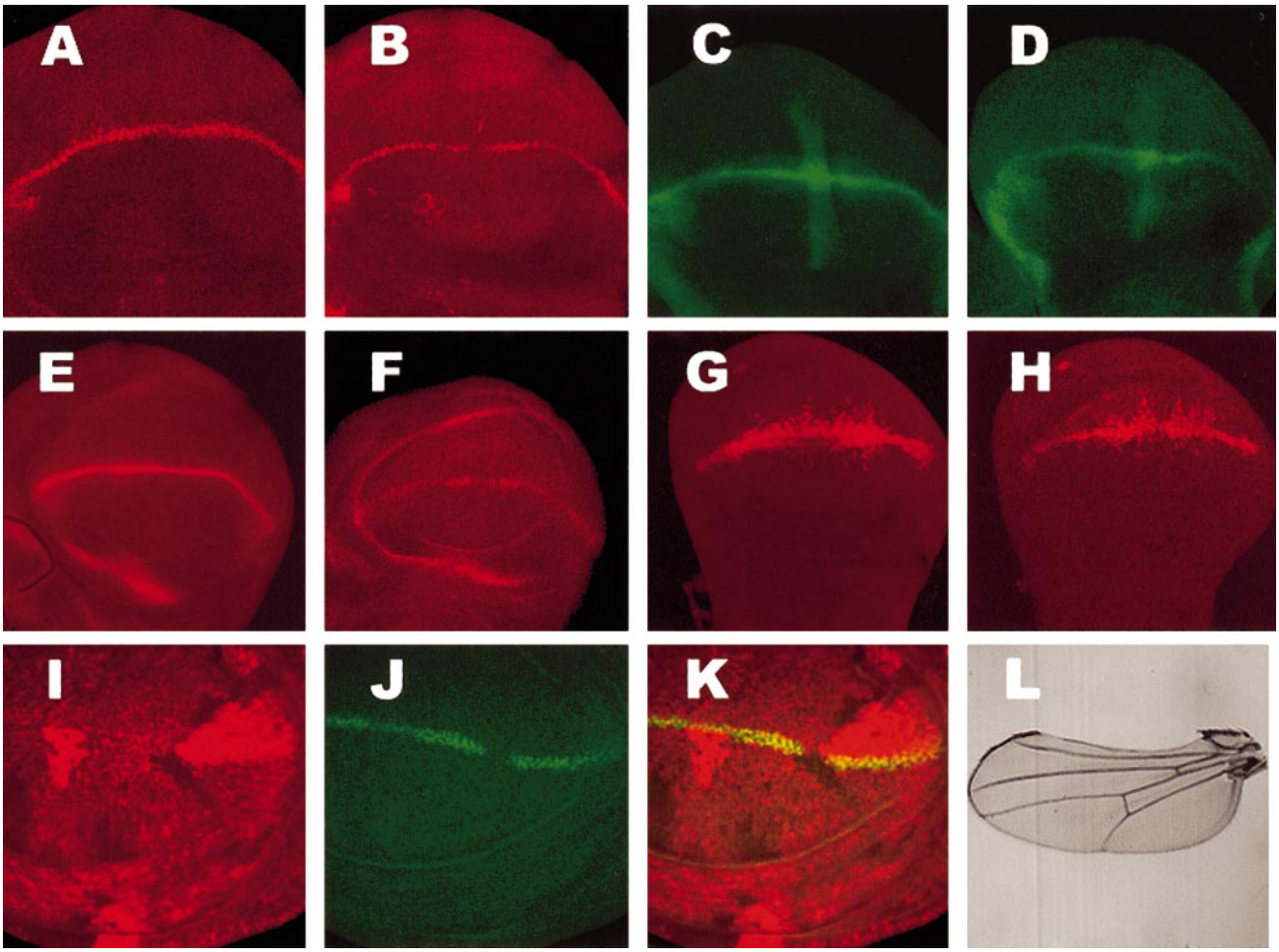

FIG. 5. Wing margin expression of the MamN truncation disrupts expression of Notch pathway targets. Late third-instar larval wing discs were stained with antibodies to Cut (A, B), β-galactosidase (C, D, G, H), or Wg (E, F). Cut expression in +/+ (w^{1118}) discs (A), and Cut expression in *C96-MamN*/+ discs (B). *LacZ* expression in *vg-LacZ*/+ discs (C), and *LacZ* expression in *vg-LacZ*/*C96-MamN* discs (D). Wg expression in +/+ discs (E), and Wg expression in *C96-MamN*/+ discs (F). *LacZ* expression in *C96-GAL4*/*UAS-LacZ* discs (G), and *LacZ* expression in *C96-MamN*/*UAS-LacZ* discs (H). Mosaic discs containing patches of mam^{IL115}/mam^{IL115} tissue were produced as described under Materials and Methods and stained with antibodies to Myc and Cut proteins. mam^{IL115}/mam^{IL115} clones are marked by the absence of Myc protein staining (I, red). Mosaic patches that cross the wing margin eliminate expression of Cut protein (J, green). Merged image (K). Some adults emerging from this experiment exhibited wing margin defects (L).

FIG. 6. Loss of expression of Notch pathway targets coincides with expression of the MamN truncation. The *blk-GAL4* construct drives along the A/P border of the wing disc (Morimura *et al.*, 1996) and was used to analyze coincidence of *MamN* expression and loss of target gene expression. Anterior is to the left in A–I. *blk-GAL4*/*UAS-MamN* discs were stained for Mam (MamN) protein (A, D, G) and either Cut (B), β-galactosidase for *vg-LacZ* (E), or Wg (H) protein. (C, F, and I) Merged images illustrating MamN and target gene expression patterns. At the margin, loss of Cut and Wg expression coincide exactly with the presence of MamN. However, *vg-LacZ* expression is evident in the posterior domain of MamN expression along the margin. The *blk-GAL4*/*UAS-MamN* combination produces very striking adult phenotypes, including duplications of scutellar macrochaetes (J), thickened wing vein 3 and a loss of material at the anterior/posterior boundary of the margin (K), and small rough eyes (L). Some eyes exhibit more significant ommatidial losses ventrally (not shown). These phenotypes can be enhanced by mutations in other Notch pathway loci. A *blk-GAL4* + *UAS-MamN* recombinant chromosome (*blk-MamN*) was constructed. The *blk-MamN* eye phenotype is enhanced by mutation of *mam* (M), mam^{IL115}/+; *blk-MamN*/+, *N* (N), N^{5419}/+; *blk-MamN*/+, and *Dl* (O), Dl^{BX9}/*blk-MamN*.

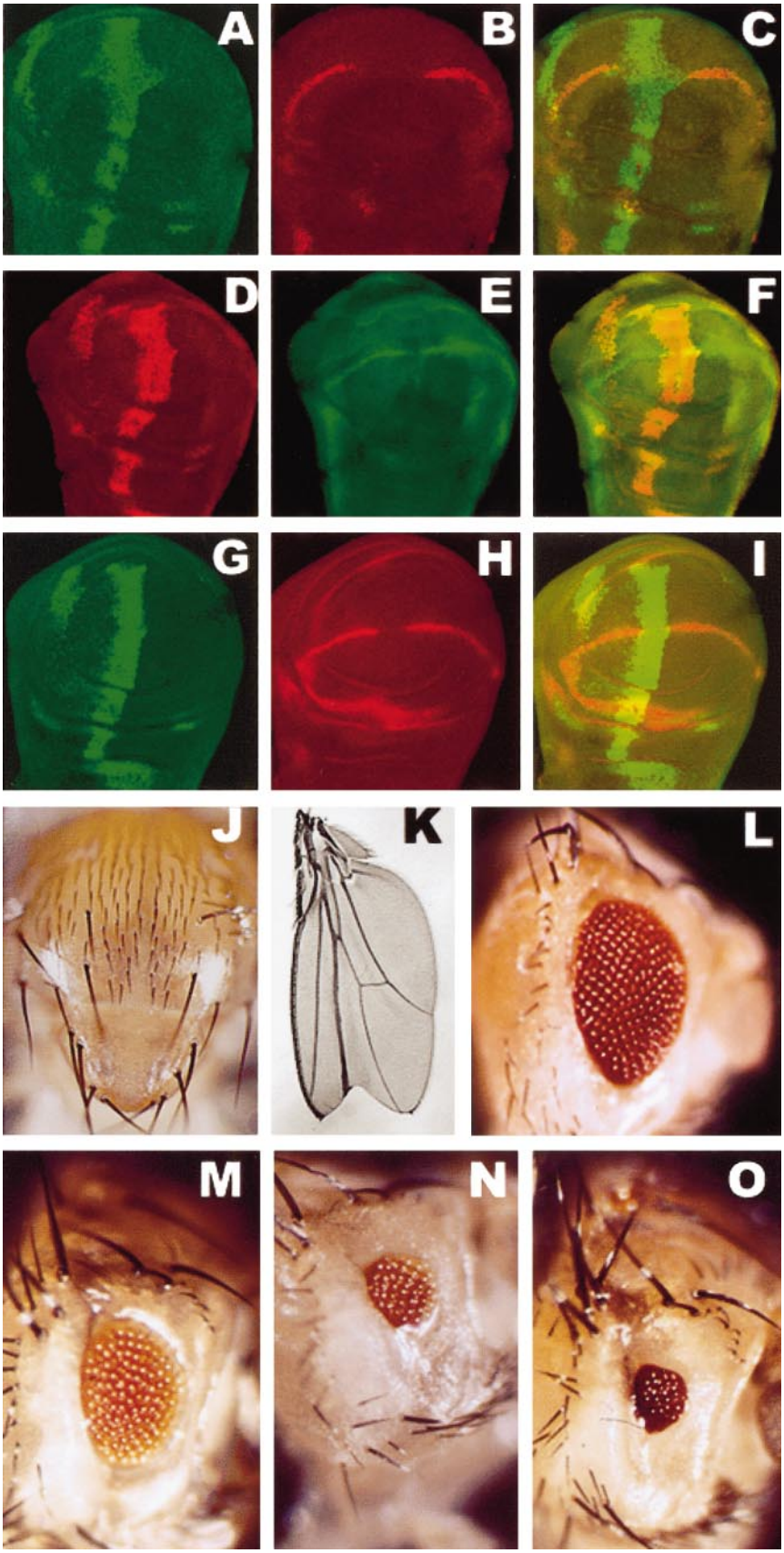

action upstream of activated Notch. However, some modifications in *C96-GAL4*-induced bristle phenotypes are observed following coexpression of *C96-MamN* with *UAS-Dl*, *UAS-Ser*, and *UAS-Su(H)* (Fig. 7 legend).

Alterations in Wg Pathway Function Modify the Mam Wing Phenotype

The wing phenotypes associated with *C96-MamN* expression are characteristic of *wg* mutations (Baker, 1988; Axelrod *et al.*, 1996), suggesting that the loss of Wg expression mediated by *C96-MamN* contributes to the phenotype. This was investigated by analyzing interactions between *C96-MamN* and mutations in Wg pathway genes. Wing enhancements are associated with wg^{CX4}/+; *C96-MamN*/+ (Fig. 8A) and arm^{1}/+; *C96-MamN*/+ (Fig. 8B) genotypes; however, these effects are observed at lower frequency and are less severe than those observed with Notch pathway mutations. No interactions are observed with mutations in *dsh*, *zw3*, or *pan* (Figs. 8C–8E). To examine genetic interaction with the Dfz2 Wg receptor, we used *UAS-GPI-Dfz2*, a truncated version of the receptor that appears to function in a dominant-negative manner (Cadigan *et al.*, 1998). The *C96-GAL4*/*UAS-GPI-Dfz2* genotype is associated with a minor wing-nicking phenotype (Fig. 8F). However, *C96-MamN*/*UAS-GPI-Dfz2* flies exhibit enhancement to variable extents, including wings that are missing significant blade material (Fig. 8G).

Overexpression of Wg pathway components partially rescues the *C96-MamN* phenotype. Expression of *UAS-Dsh* (Figs. 7O and 7P) or $UAS\text{-}Arm^{S10}$, an activated form of Arm (Van de Wetering *et al.*, 1997) (Figs. 7U and 7V), restores most of the wing margin. However, expression of *UAS-Dfz2* (Figs. 7M and 7N), *UAS-Arm* (Fig. 7S and 7T), or *UAS-dTCF* (Figs. 7W and 7X) does not rescue. *UAS-Zw3* enhances the wing phenotype (Figs. 7Q and 7R).

Interactions between *C96-MamN* and a *cut* mutation are also observed (Figs. 8H and 8I), consistent with reports of genetic interactions between *mam* and *cut* (Morcillo *et al.*, 1996). However, a deletion that removes the *vg* locus does not detectably interact with *C96-MamN* (data not shown).

DISCUSSION

Overexpression of a Truncated Mam Protein Elicits Loss-of-Function Notch Pathway Phenotypes

Genetic studies have implicated *mam* as an integral component of the Notch pathway in *Drosophila* (Lehmann *et al.*, 1983; Dietrich and Campos-Ortega, 1984; Xu and Artavanis-Tsakonas, 1990; Xu *et al.*, 1990; Verheyen *et al.*, 1996). However, detailed studies of *mam* function during processes known to involve Notch signaling have not been performed. We have demonstrated that targeted overexpression of truncated versions of the Mam protein under *GAL4* regulation in transgenic flies produces distinct mutant phenotypes. Based on several criteria, these phenotypes appear to reproduce those associated with loss-of-function mutations in Notch pathway genes. This system also provided evidence of Mam function upstream of Notch activation during wing margin formation.

A bristle organ in the notum arises from an SOP cell that is specified within a proneural cluster (Hartenstein and Posakony, 1989). Mam truncations driven by *GAL4* in notal regions under *309*, *pnr*, and *blk* (*dpp*) control elicit effects on bristle development consistent with reductions in Notch signaling. Notal MamN expression results in multiple macrochaetes at each macrochaete site and supernumerary microchaete SOPs, indicating a failure in Notch-mediated lateral inhibition in bristle proneural clusters. We also observe transformations of socket to shaft and of all four bristle progeny to the neuronal cell fate, indicating that expression of truncated Mam interferes with Notch signaling during later stages of bristle development as well.

During wing development, the Notch pathway is required for delimiting veins (de Celis, 1997; Huppert *et al.*, 1997) and proper margin formation and growth (Rulifson and Blair, 1995; Neumann and Cohen, 1996; Kim *et al.*, 1996; de Celis and Bray, 1997; Micchelli *et al.*, 1997; Fleming *et al.*, 1997). Expression of truncated Mam within the provein of wing vein 3, near the A/P compartment boundary, results in increased numbers of vein cells, a Notch pathway loss-of-function phenotype (de Celis, 1997; Huppert *et al.*, 1997). When expressed at the wing margin, truncated Mam produces nicking and bristle loss phenotypes similar to those associated with mutations in *N* and

FIG. 7. Rescue of the *C96-MamN* truncation wing-nicking phenotype through overexpression of components of the Notch and Wg pathways. The *C96-MamN/TM3* strain was crossed with strains carrying Notch and Wg pathway transgenes under *GAL4-UAS* regulation, and progeny were scored for modification of the *C96-MamN* wing-nicking phenotype. In each pair of images the left shows wings obtained from adults carrying the *UAS*-transgene combined with the *C96-GAL4* driver; the right represents the same *UAS* transgene in combination with the *C96-MamN* chromosome. *UAS-Dl/+; C96-GAL4/+* wings show distal anterior margin bristle duplications and proximal bristle loss and appear slightly convex at the dorsal surface (A). *UAS-Dl/+; C96-MamN/+* wings show significant rescue of margin nicking. Additionally, these wings contain bristle duplications along the entire anterior margin (B). *UAS-Ser/+; C96-GAL4/+* wings show minor bristle duplications near the distal anterior margin (C). *UAS-Ser/+; C96-MamN/+* wings show weak and highly variable rescue of margin nicking. Nicking is evident along the anterior or posterior margin in most wings. Although not evident in the image displayed, these wings can exhibit a slight suppression of bristle duplication (D). $UAS\text{-}N^{act}$/+; *C96-GAL4/+* wings show bristle loss and double sockets along the

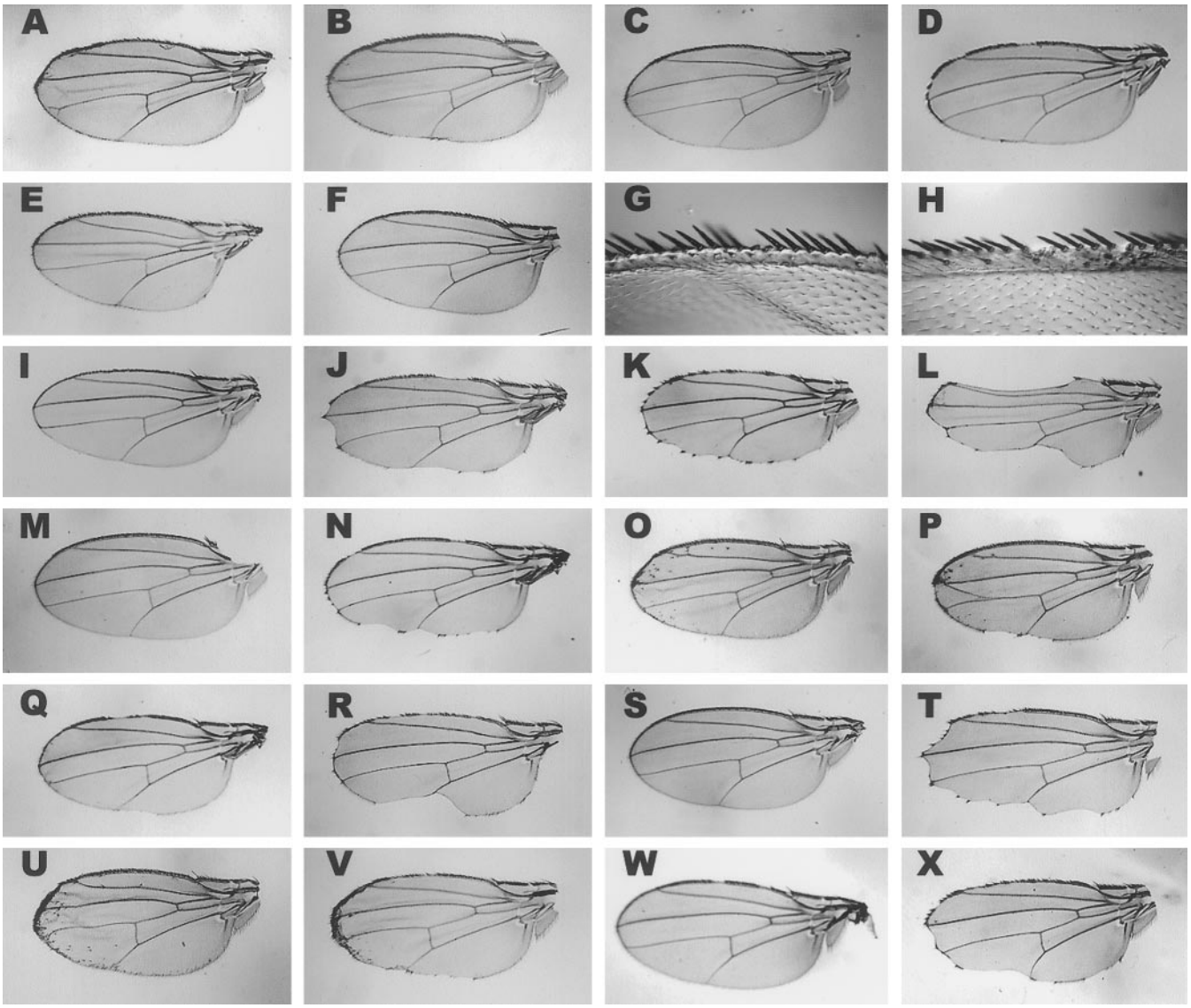

anterior margin and appear convex at the dorsal surface (E, G; G is a higher magnification image of E). *UAS-N^{act}/+; C96-MamN/+* wings exhibit nearly complete rescue of margin nicks (F). However, the bristle loss and double-socket phenotype are still evident (H, higher magnification image of F). *UAS-Su(H)/+; C96-GAL4/+* wings show extensive bristle loss and double sockets at the anterior margin (I). *UAS-Su(H)/+; C96-MamN/+* wings do not show rescue of margin nicking, and in some cases margin loss is enhanced and includes wing blade material. Although the bristle loss and double-socket phenotype persist, a slight restoration of bristles is evident within regions of intact margin (J). *UAS-H/+; C96-GAL4/+* wings show significant bristle loss and nicking at the margin (K). *UAS-H/+; C96-MamN/+* wings exhibit extensive loss of blade material at anterior and posterior regions (L). *UAS-Dx/C96-GAL4* wings appear normal and *UAS-Dx/C96-MamN* wings do not show rescue (data not shown). *UAS-Dfz2/+; C96-GAL4/+* wings appear normal (M). *UAS-Dfz2/+; C96-MamN/+* wings do not show rescue (N). *UAS-Dsh/C96-GAL4* wings show additional margin bristles and some ectopic bristles on the wing blade near the margin (O). *UAS-Dsh/C96-MamN* wings show partial rescue of margin nicks (P). *UAS-Zw3/+; C96-GAL4/+* wings show nicks and bristle loss at the margin (Q). *UAS-Zw3/+; C96-MamN/+* wings exhibit enhanced nicking at the margin (R). Wild-type Arm: *UAS-Arm/+; C96-GAL4/+* wings appear normal (S). *UAS-Arm/+; C96-MamN/+* wings do not show rescue (T). Activated Arm: *UAS-Arm^{S10}/+; C96-GAL4/+* wings show additional margin bristles and ectopic bristles, as well as bubbles at the distal end (U). *UAS-Arm^{S10}/+; C96-MamN/+* wings exhibit similar disturbances; however, significant rescue of the wing-nicking phenotype is evident (V). *UAS-dTCF/+; C96-GAL4/+* wings show minor wing nicking (W). *UAS-dTCF/+; C96-MamN/+* wings do not show rescue (X).

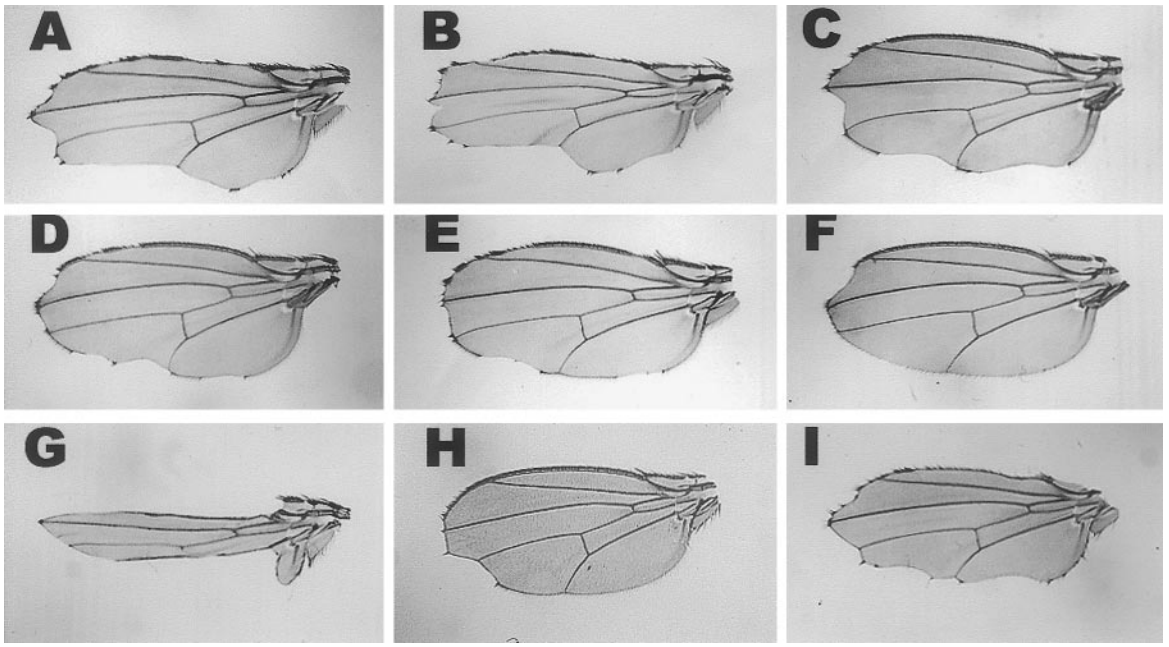

FIG. 8. The *C96-MamN* truncation wing phenotype is modified by mutations in Wg pathway genes and *cut*. Strains containing mutations in the Wg pathway or *cut* were crossed to *C96-MamN/TM3, Sb* flies and scored for wing phenotypes. Wings from wg^{CX4}/+; *C96-MamN*/+ flies show an enhanced phenotype that is partially penetrant, including loss of additional blade material along the posterior margin and bristle loss along the anterior margin (A). A low percentage of more severe strap wings is also observed (data not shown). Wings from arm^{1}/+; *C96-MamN*/+ flies exhibit enhancements of the *C96-MamN*/+ phenotype similar to those induced by a *wg* mutation (B). These phenotypes are also incompletely penetrant. Wings from dsh^{V26}/+; *C96-MamN*/+ (C), $zw3^{M11\text{-}1}$/+; *C96-MamN*/+ (D), and pan^{13a}/*C96-MamN* flies (E) do not exhibit modifications of the *C96-MamN*/+ phenotype. To assess genetic interactions with the Dfz2 Wg receptor, we utilized a *UAS-GPI-Dfz2* strain encoding a truncated form of Dfz2. *UAS-GPI-Dfz2* elicits dominant-negative effects under appropriate *GAL4* regulation (Cadigan *et al.,* 1998). When this construct is driven in the *C96-GAL4/UAS-GPI-Dfz2* genotype, virtually all flies contain wings with anterior terminal nicking (F). Wings from *C96-MamN/UAS-GPI-Dfz2* exhibit a wide range of enhanced phenotypes, including severe loss of blade material (G). Wings from cut^{53d}/*Y* flies exhibit a minor margin-nicking phenotype (H). Wings from cut^{53d}/*Y; C96-MamN*/+ flies exhibit enhanced wing phenotypes (I).

wg (Axelrod *et al.*, 1996). Additionally, MamN expression reduces the margin expression of *wg*, *cut*, and *vg*. Analysis of *mam/mam* mosaic clones demonstrates that the wing margin effects of MamN represent *mam* loss-of-function phenotypes. Finally, the MamN-induced wing margin phenotypes are modified by mutations in the Notch and Wg pathways.

Most Notch pathway mutations exhibit a synergistic interaction with the *C96-MamN* genotype; however, $E(spl)^{8D06}$, which deletes the *E(spl)* complex and *groucho*, does not exhibit interactions. This is consistent with the observation that the *E(spl)* complex does not play a major role in wing margin formation (de Celis *et al.*, 1996), although effects on Cut expression within either *E(spl)* or *groucho* mutant clones have been reported recently (Ligoxygakis *et al.*, 1999). In contrast, loss-of-function for *Su(H)* along the wing margin is associated with defects (de Celis *et al.*, 1996), yet we do not observe interactions between loss-of-function *Su(H)* alleles and *C96-MamN*. This may indicate that Su(H) protein is normally present in substantial excess at the margin, compared to the levels required for wild-type function. Interestingly, a gain-of-function allele, $Su(H)^{S5}$, enhances the *C96-MamN* wing phenotype. Similar genetic interactions were observed during studies of $Su(H)^{S5}$ and the loss-of-function mam^{IL115} allele (Fortini and Artavanis-Tsakonas, 1994). Although the basis for these interactions is unclear, genetic data indicate that *Su(H)* gain-of-function mutations may not simply result in an increase in wild-type activity (Fortini and Artavanis-Tsakonas, 1994). Analyses of mammalian homologs of Su(H) have shown that the protein functions as a repressor until it complexes with a coactivator, such as EBNA2 (Hsieh and Hayward, 1995) or the intracellular domain of Notch (Jarriault *et al.*, 1995). *Su(H)* gain-of-function alleles could encode aberrant proteins with novel activities, such as elevated repression, that perturb Notch pathway signaling; when such a protein is present, reduction in *mam* function may produce a synergistic effect.

Wg pathway interactions with *C96-MamN* are observed with mutations in *wg* and *arm* and with coexpression of

several downstream effectors. Such interactions presumably result from the depression of Wg expression at the margin, associated with expression of the MamN truncation. Wg pathway action is initiated by the interaction of Wg and Dfz2. This interaction leads to activation of Dsh, inhibition of Zw3, and subsequent stabilization of Arm protein. Arm then functions in the nucleus as a coactivator with the DNA-binding protein dTCF (van de Wetering *et al.,* 1997). The basis for the absence of *C96-MamN* genetic interaction with *dsh, zw3,* or *dTCF* mutations is unknown, but may be related to the basal expression levels of these components, as suggested above for Su(H). Additionally, Wg pathway function is influenced by other regulatory inputs (Peifer, 1999) and involves enzymatic activities (Siegfried *et al.,* 1994) that may be subject to posttranslational modes of regulation.

Genetic Epistasis Analyses Suggest an Early Function for Mam within the Notch Pathway during Wing Margin Formation

One of the central questions concerning the role of Mam is its site(s) of action within the Notch pathway. Previous studies of embryonic neurogenesis indicated that Mam is required upstream of Notch activity for lateral inhibition (de la Concha *et al.,* 1988; Lieber *et al.,* 1993). In contrast, the data of Schuldt and Brand (1999) indicate that Mam can act downstream of Notch later during CNS development, when specific neuronal cell fates are established by the pathway (Skeath and Doe, 1998; Buescher *et al.,* 1998). Our studies largely support a role for Mam upstream of Notch activation during wing margin formation. Overexpression of Delta or activated Notch, and to a minor extent Serrate, rescues the wing-nicking phenotype induced by the MamN truncation. One hypothesis suggested by these observations, that Mam positively regulates expression of Notch ligands, particularly Delta, is being investigated. Although we favor the hypothesis that Mam acts upstream of Notch activation during wing margin epithelium formation, our data do not exclude a role for Mam at other sites in the pathway during this process. For example, expression of MamN is unlikely to produce a total loss-of-function *mam* phenotype. Therefore, high levels of upstream effectors may be able to surmount partial blockage of Mam function, even if Mam functions downstream of Notch activation. Furthermore, the interpretation of epistasis data can be problematic given the existence of feedback regulation within the Notch pathway (de Celis and Bray, 1997; Huppert *et al.,* 1997; Micchelli *et al.,* 1997) and interpathway interactions involving the Notch pathway (Axelrod *et al.,* 1996; Karim *et al.,* 1996; Price *et al.,* 1997). Given such complexities, it is conceivable that a "downstream" perturbation can manifest effects at one or more points "upstream" in the pathway. For example, it appears that Wg, a target of the Notch pathway, positively regulates Notch ligand expression during wing margin formation (Micchelli *et al.,* 1997, de Celis and Bray, 1997). Therefore, some phenotypic effects of Mam truncations could be mediated through a reduction of ligand activity, an indirect effect of depressed Wg levels.

Given its role as an effector of Notch pathway function in various contexts (Fortini and Artavanis, 1994; Jennings *et al.,* 1994; Bailey and Posakony, 1995; Lecourtois and Schweisguth, 1995; Neumann and Cohen, 1996), it is interesting that Su(H) overexpression does not rescue wing-nicking induced by Mam truncation expression. This result might be explained by the observation that Su(H)-related proteins require a coactivator, such as the Notch intracellular domain, for transcriptional activation functions (Hsieh and Hayward, 1995). Since the MamN truncation appears to compromise Notch pathway activity prior to Notch activation, excess Su(H) alone may not be sufficient to rescue MamN effects on wing margin epithelium formation.

Finally, in the context of bristle formation at the wing margin we observe that the MamN truncation does not modify effects produced by overexpression of activated Notch, consistent with a role for Mam upstream of Notch activation. However, the truncation can modify bristle effects associated with overexpression of Delta, Serrate, and Su(H). This may indicate a role for Mam downstream of Notch activation during bristle formation at the margin or lower levels of GAL4-UAS-mediated expression of Delta, Serrate, and Su(H) in developing bristles versus wing margin epithelium. In any case, these data imply that expression of activated Notch may not be equivalent to expression of excess quantities of Notch ligands or Su(H) within the context of wing margin bristle development.

Mam Truncations May Behave as Dominant-Negative Proteins

Mam contains clusters of charged amino acids and associates with transcriptionally active and repressed chromosomal regions (Bettler *et al.,* 1996), indicative of a genetic regulatory function. Dominant-negative behaviors associated with truncated transcription factors that retain DNA-binding activity have been reported (Bohmann *et al.,* 1994; Singh *et al.,* 1998; Stoffers *et al.,* 1998), and it is likely that some of these effects derive from competition between mutant and wild-type proteins. Therefore, ineffective Mam truncations may compete with wild-type Mam proteins and poison transcription complexes that are essential for Notch pathway function. Elimination of the carboxy-terminal acidic charge cluster of Mam elicits very minor effects. In contrast, a truncation that eliminates approximately the carboxy-terminal third of Mam (MamN) induces significant phenotypic effects when overexpressed. The MamN truncation removes two of three runs of alternating glycine and valine, a polyalanine run, and other homopolymer runs distributed within nonrepetitive Mam sequences. It remains to be determined which, if any, of these sequences serves an effector role in Mam. The MamH truncation produces phenotypes qualitatively similar to those induced by MamN, despite the loss of additional Mam sequences up

to the basic charge cluster. This indicates that an important determinant for the production of these phenotypes resides in or near the basic charge cluster. Given the high penetrance of the phenotypes it should be possible to identify residues within the truncation essential for these effects. For example, several amino acids within the Mam basic domain are shared by the DNA binding domains of bZip proteins (Bettler *et al.*, 1996). If alteration of such residues in a Mam truncation were to eliminate phenotypic effects and chromosomal association, it would provide indirect support for the hypothesis that Mam functions through an association with DNA.

ACKNOWLEDGMENTS

We are most appreciative to the colleagues who generously supplied antisera and *Drosophila* strains, including G. Boulianne, S. Artavanis-Tsakonas, K. Matsuno, M. Hoffman, B. Hay, G. Morata, K. Bhat, J. Axelrod, R. Fleming, J. Posakony, M. Peifer, A. Bejsovec, S. Carroll, T. Xu, N. Perrimon, and J. Jack. This work was supported by NSF IBN 9630161, IBN 9904411 (B.Y.), and NIH GM 33291 (M.A.T.M) B.Y. also acknowledges support from the Ammerman Foundation.

REFERENCES

Artavanis-Tsakonas, S., Matsuno, K., and Fortini, M. E. (1995). Notch signaling. *Science* **268,** 225–232.

Axelrod, J. D., Matsuno, K., Artavanis-Tsakonas, S., and Perrimon, N. (1996). Interaction between *wingless* and *Notch* signaling pathways mediated by *disheveled*. *Science* **271,** 1826–1832.

Bailey, A. M., and Posakony, J. W. (1995). Suppressor of Hairless directly activates transcription of *Enhancer of split* complex genes in response to Notch receptor activity. *Genes Dev.* **9,** 2609–2622.

Baker, N. E. (1988). Embryonic and imaginal requirements for *wingless*, a segment-polarity gene in *Drosophila*. *Dev. Biol.* **125,** 96–108.

Baker, N. E., and Yu, S. Y. (1997). Proneural function of neurogenic genes in the developing *Drosophila* eye. *Curr. Biol.* **7,**122–132.

Bang, A., and Posakony, J. W. (1992). The *Drosophila* gene *Hairless* encodes a novel basic protein that controls alternative cell fates in adult sensory organ development. *Genes Dev.* **6,** 1752–1769.

Bang, A. G., Bailey, A., and Posakony, J. W. (1995). *Hairless* promotes stable commitment to the sensory organ precursor cell fate by negatively regulating the activity of the *Notch* signaling pathway. *Dev. Biol.* **172,** 479–494.

Bender, L. B., Kooh, P. J., and Muskavitch, M. A. T. (1993). Complex function and expression of *Delta* during *Drosophila* oogenesis. *Genetics* **133,** 967–978.

Bettler, D., Schmid, A., and Yedvobnick, B. (1991). Early ventral expression of the neurogenic locus *mastermind*. *Dev. Biol.* **144,** 436–439.

Bettler, D., Pearson, S., and Yedvobnick, B. (1996). The nuclear protein encoded by the *Drosophila* neurogenic gene *mastermind* is widely expressed and associates with specific chromosomal sites. *Genetics* **143,** 859–875.

Bohmann, D., Ellis, M. C., Staszewski, L. M., and Mlodzik, M. (1994). *Drosophila* Jun mediates Ras-dependent photoreceptor determination. *Cell* **78,** 973–986.

Brand, A. H., and Perrimon, N. (1993). Targeted gene expression as a means of altering cell fates and generating dominant phenotypes. *Development* **118,** 401–415.

Brand, M., and Campos-Ortega, J. A. (1990). Second site modifiers of the *split* mutation of *Notch* define genes involved in neurogenesis in *Drosophila melanogaster*. *Wilhelm Roux's Arch. Dev. Biol.* **198,** 275–285.

Brennan, C. A., Ashburner, M., and Moses, K. (1998). Ecdysone pathway is required for furrow progression in the developing *Drosophila* eye. *Development* **125,** 2653–2664.

Buescher, M., Yeo, S. L., Udolph, G., Zavortink, M., Yang, X., Tear, G., and Chia, W. (1998). Binary sibling neuronal cell fate decisions in the *Drosophila* embryonic central nervous system are nonstochastic and require inscuteable-mediated asymmetry of ganglion mother cells. *Genes Dev.* **12,** 1858–1870.

Cadigan, K. M., Fish, M. P., Rulifson, E. J., and Nusse, R. (1998). Wingless repression of *Drosophila frizzled 2* expression shapes the Wingless morphogen gradient in the wing. *Cell* **93,** 767–777.

Cagan, R. L., and Ready, D. F. (1989). Notch is required for successive cell fate decisions in the developing *Drosophila* retina. *Genes Dev.* **3,** 1099–1112.

Carroll, S. B., and Whyte, J. S. (1989). The role of the *hairy* gene during *Drosophila* morphogenesis: Stripes in imaginal discs. *Genes Dev.* **3,** 905–916.

Coffman, C. R., Skoglund, P., Harris, W. A., and Kintner, C. R. (1993). Expression of an extracellular deletion of Xotch diverts cell fate in Xenopus embryos. *Cell* **73,** 659–671.

Corbin, V., Michelson, A. M., Abmayr, S. M., Neel, V., Alcomo, E., Maniatis, T., and Young, M. W. (1991). A role for the *Drosophila* neurogenic genes in mesoderm differentiation. *Cell* **67,** 311–323.

de Celis, J. F. (1997). Expression and function of decapentaplegic and thick veins during the differentiation of the veins in the *Drosophila* wing. *Development* **124,** 1007–1018.

de Celis, J. F., de Celis, J., Ligoxygakis, P., Preiss, A., Delidakis, C., and Bray, S. (1996). Functional relationships between *Notch*, *Su(H)* and the bHLH genes of the *E(spl) complex:* The *E(spl)* genes mediate only a subset of Notch activities during imaginal development. *Development* **122,** 2719–2728.

de Celis, J. F., and Bray, S. (1997). Feed-back mechanisms affecting Notch activation at the dorsoventral boundary in the *Drosophila* wing. *Development* **124,** 3241–3251.

de la Concha, A., Dietrich, V., Weigel, D., and Campos-Ortega, J. A. (1988). Functional interactions of neurogenic genes of *Drosophila melanogaster*. *Genetics* **118,** 499–508.

Dietrich, U., and Campos-Ortega, J. A. (1984). The expression of neurogenic loci in imaginal epidermal cells of *Drosophila melanogaster*. *J. Neurogenet.* **1,** 315–322.

Fleming, R. J., Gu, Y., and Hukriede, N. A. (1997). Serrate-mediated activation of Notch is specifically blocked by the product of the gene fringe in the dorsal compartment of the *Drosophila* wing imaginal disc. *Development* **124,** 2973–2981.

Fortini, M. E., Rebay, I., Caron, L. A., and Artavanis-Tsakonas, S. (1993). An activated Notch receptor blocks cell-fate commitment in the developing *Drosophila* eye. *Nature* **365,** 555–557.

Fortini, M. E., and Artavanis-Tsakonas, S. (1994). The *Suppressor of Hairless* protein participates in *Notch* receptor signaling. *Cell* **79,** 273–282.

Freeman, M. (1996). Reiterative use of the EGF receptor triggers differentiation of all cell types in the *Drosophila* eye. *Cell* **87,** 651–660.

Gallyas, F., Göres, T., and Merchenthaler, I. (1982). High-grade intensification of the end-product of the diaminobenzidine reac-

tion for peroxidase histochemistry. *J. Histochem. Cytochem.* **30,** 183–184.

Greenwald, I., and Rubin, G. M. (1992). Making a difference: The role of cell–cell interactions in establishing separate identities for equivalent cells. *Cell* **68,** 271–282.

Gridley, T. (1997). Notch signaling in vertebrate development and disease. *Mol. Cell. Neurosci.* **9,** 103–108.

Gustafson, K., and Boulianne, G. L. (1996). Distinct expression patterns detected within individual tissues by the GAL4 enhancer trap technique. *Genome* **39,** 174–182

Hartenstein, V. (1988). Development of *Drosophila* larval sensory organs: Spatiotemporal pattern of sensory neurons, peripheral axonal pathways, and sensilla differentiation. *Development* **102,** 869–886.

Hartenstein, V., and Campos-Ortega, J. A. (1986). The peripheral nervous system of mutants of early neurogenesis in *Drosophila melanogaster. Wilhelm Roux's Arch. Dev. Biol.* **195,** 210–221.

Hartenstein, V., and Posakony, J. W. (1989). Development of adult sensilla on the wing and notum of *Drosophila* melanogaster. *Development* **107,** 389–405.

Hartenstein, V., and Posakony, J. W. (1990). A dual function of the *Notch* gene in *Drosophila* sensillum development. *Dev. Biol.* **142,** 13–30.

Hartenstein, A. Y., Rugendorff, A., Tepass, U., and Hartenstein, V. (1992). The function of the neurogenic genes during epithelial development in the *Drosophila* embryo. *Development* **116,** 1203–1220.

Heitzler, P., Haenlin, M., Ramain, P., Calleja, M., and Simpson, P. (1996a). A genetic analysis of *pannier,* a gene necessary for viability of dorsal tissues and bristle positioning in *Drosophila. Genetics* **143,** 1271–1286.

Heitzler, P., Bourouis, M., Ruel, L., Carteret, C., and Simpson, P. (1996b). Genes of the *Enhancer of split* and *achaete–scute* complexes are required for a regulatory loop between Notch and Delta during lateral signaling in *Drosophila. Development* **122,** 161–171.

Hsieh, J. J. D., and Hayward, S. D. (1995). Masking of the CBF1/RBPJk transcriptional repression domain by Epstein–Barr virus EBNA2. *Science* **268,** 560–563.

Hubbard, E. J., Dong, Q., and Greenwald, I. (1996). Evidence for physical and functional association between EMB-5 and LIN-12 in *C. elegans. Science* **273,** 112–115.

Huppert, S. S., Jacobsen, T. L., and Muskavitch, M. A. (1997). Feedback regulation is central to Delta–Notch signaling required for *Drosophila* wing vein morphogenesis. *Development* **124,** 3283–3291.

Jarriault, S., Brou, C., Logeat, F., Schroeter, E. H., Kopan, R., and Israel, A. (1995). Signaling downstream of activated mammalian Notch. *Nature* **377,** 355–358.

Jennings, B., Preiss, A., Delidakis, C., and Bray, S. (1994). The Notch signaling pathway is required for *Enhancer of split* HLH protein expression during neurogenesis in the *Drosophila* embryo. *Development* **120,** 3537–3548.

Karim, F. D., Chang, H. C., Therrien, M., Wassarman, D. A., Laverty, T., and Rubin, G. M. (1996). A screen for genes that function downstream of Ras1 during *Drosophila* eye development. *Genetics* **143,** 315–329.

Kim, J., Sebring, A., Esch, J. J., Kraus, M. E., Vorwerk, K., Magee, J., and Carroll, S. B. (1996). Integration of positional signals and regulation of wing formation and identity by *Drosophila vestigial* gene. *Nature* **382,** 133–138.

Lecourtois, M., and Schweisguth, F. (1995). The neurogenic Suppressor of Hairless DNA-binding protein mediates the transcriptional activation of the *Enhancer of split* complex genes triggered by Notch signaling. *Genes Dev.* **9,** 2598–2608.

Lehmann, R. F., Jimenez, W., Dietrich, U., and Campos-Ortega, J. A. (1983). On the phenotype and development of mutants of early neurogenesis in *D. melanogaster. Wilhelm Roux's Arch. Dev. Biol.* **192,** 62–74.

Levitan, D., and Greenwald, I. (1995). Facilitation of *lin-12*-mediated signaling by *sel-12,* a *Caenorhabditis elegans* S182 Alzheimer's disease gene. *Nature* **377,** 351–354.

Lieber, T., Kidd, S., Alcamo, E., Corbin, V., and Young, M. W. (1993). Antineurogenic phenotypes induced by truncated Notch proteins indicate a role in signal transduction and may point to a novel function for Notch in nuclei. *Genes Dev.* **7,** 1949–1965.

Ligoxygakis, P., Bray, S. J., Apidianakis, Y., and Delidakis, C. (1999). Ectopic expression of individual *E(spl)* genes has differential effects on different cell fate decisions and underscores the biphasic requirement for Notch activity in wing margin establishment in Drosophila. *Development* **126,** 2205–2214.

Lindsley, D. L., and Zimm, G. G. (1992). "The genome of *Drosophila melanogaster*" Academic Press, San Diego.

Liposits, Z. S., Sétáló, G. Y., and Lerkó, B. F. (1984). Application of the silver-gold intensified 3,3-diaminobenzidine chromatin to the light and electron microscopic detection of the luteinizing hormone releasing hormone detection system of the rat brain. *Neuroscience* **13,** 513–525.

Lyman, D., and Yedvobnick, B. (1995). *Drosophila Notch* receptor activity suppresses *Hairless* function during adult external sensory organ development. *Genetics* **141,** 1491–1505.

Maier, D., Stumm, G., Kuhn, K., and Preiss, A. (1992). *Hairless,* a *Drosophila* gene involved in neural development, encodes novel, serine rich protein. *Mech. Dev.* **38,** 143–150.

Majumdar, A., Nagaraj, R., and Banerjee, U. (1997). *strawberry notch* encodes a conserved nuclear protein that functions downstream of Notch and regulates gene expression along the developing wing margin of *Drosophila. Genes Dev.* **11,** 1341–1353.

Masucci, J. D., Miltenberger, R. J., and Hoffmann, F. M. (1990). Pattern-specific expression of the *Drosophila decapentaplegic* gene in imaginal disks is regulated by 3′ cis-regulatory elements. *Genes Dev.* **4,** 2011–2023.

Matsuno, K., Go, M. J., Sun, X., Eastman, D. S., and Artavanis-Tsakonas, S. (1997). Suppressor of Hairless-independent events in Notch signaling imply novel pathway elements. *Development* **124,** 4265–4273.

Micchelli, C. A., Rulifson, E. J., and Blair, S. S. (1997). The function and regulation of Cut expression on the wing margin of *Drosophila:* Notch, Wingless and a dominant negative role for Delta and Serrate. *Development* **124,** 1485–1495.

Morcillo, P., Rosen, C., and Dorsett, D. (1996). Genes regulating the remote wing margin enhancer in the *Drosophila cut* locus. *Genetics* **144,** 1143–1154.

Morimura, S., Maves, L., Chen, Y., and Hoffmann, F. M. (1996). *decapentaplegic* overexpression affects *Drosophila* wing and leg imaginal disc development and *wingless* expression. *Dev. Biol.* **177,** 136–151.

Neumann, C. J., and Cohen, S. M. (1996). A hierarchy of cross-regulation involving Notch, Wingless, Vestigial and Cut organizes the dorsal/ventral axis of the *Drosophila* wing. *Development* **122,** 3477–3485.

Newfeld, S., Schmid, A., and Yedvobnick, B. (1993). Homopolymer length variation in the *Drosophila* gene *mastermind*. *J. Mol. Evol.* **37,** 483–495.

Oellers, N., Dehio, M., and Knust, E. (1994). bHLH proteins encoded by the *Enhancer of Split* complex of *Drosophila* negatively interfere with transcriptional activation mediated by proneural genes. *Mol. Gen. Genet.* **244,** 465–473.

Parks, A. L., and Muskavitch, M. A. T. (1993). *Delta* function is required for bristle organ determination and morphogenesis in *Drosophila*. *Dev. Biol.* **157,** 484–496.

Parks, A. L., Turner, F. R., and Muskavitch, M. A. T. (1995). Relationships between complex Delta expression and the specification of retinal cell fates during *Drosophila* eye development. *Mech. Dev.* **50,** 201–216.

Parks, A. L., Huppert, S. S., and Muskavitch, M. A. T. (1997). The dynamics of neurogenic signaling underlying bristle development in *Drosophila melanogaster*. *Mech. Dev.* **63,** 61–74.

Parody, T. R., and Muskavitch, M. A. T. (1993). The pleiotropic function of *Delta* during postembryonic development of *Drosophila melanogaster*. *Genetics* **135,** 527–539.

Paroush, Z., Finley, R. L., Kidd, T., Wainwright, S. M., Ingham, P. I., Brent, R., and Ish-Horowicz, D. (1994). Groucho is required for *Drosophila* neurogenesis, segmentation and sex determination and interacts directly with Hairy-related bHLH proteins. *Cell* **79,** 805–815.

Peifer, M. (1999). Neither straight nor narrow. *Nature* **400,** 213–215.

Posakony, J. W. (1994). Nature versus nurture: Asymmetric cell divisions in *Drosophila* bristle development. *Cell* **76,** 415–418.

Price, J. V., Savenye, E. D., Lum, D., and Breitkreutz, A. (1997). Dominant enhancers of *Egfr* in *Drosophila melanogaster:* Genetic links between the Notch and Egfr signaling pathways. *Genetics* **147,** 1139–1153.

Robbins, J., Dilworth, S. M., Laskey, R. A., and Dingwall, C. (1991). Two interdependent basic domains in nucleoplasmin nuclear targeting sequence: Identification of a class of bipartite nuclear targeting sequence. *Cell* **64,** 615–623.

Rooke, J., Pan, D., Xu, T., and Rubin, G. M. (1996). KUZ, a conserved metalloprotease–disintegrin protein with two roles in *Drosophila* neurogenesis. *Science* **273,** 1227–1231.

Rubin, G. M., and Spradling, A. C. (1982). Genetic transformation of *Drosophila* with transposable element vectors. *Science* **218,** 348–353.

Rulifson, E. J., and Blair, S. S. (1995). Notch regulates *wingless* expression and is not required for reception of the paracrine *wingless* signal during wing margin neurogenesis in *Drosophila*. *Development* **121,** 2813–2824.

Ruohola, H., Bremer, K. A., Baker, D., Swedlow, J. R., Jan, L. Y., and Jan, Y. N. (1991). Role of neurogenic genes in establishment of follicle cell fate and oocyte polarity during oogenesis in *Drosophila*. *Cell* **66,** 433–449.

Schmid, A., Tinley, T., and Yedvobnick, B. (1996). Transcription of the neurogenic gene *mastermind* during *Drosophila* development. *J. Exp. Zool.* **274,** 207–220.

Schuldt, A. J., and Brand, A. H. (1999). Mastermind acts downstream of Notch to specify neuronal cell fates in the *Drosophila* central nervous system. *Dev. Biol.* **205,** 287–295.

Schweisguth, F., and Posakony, J. W. (1994). Antagonistic activities of *Suppressor of Hairless* and *Hairless* control alternative cell fates in the *Drosophila* adult epidermis. *Development* **120,** 1433–1441.

Siegfried, E., Wilder, E. L., and Perrimon, N. (1994). Components of *wingless* signaling in *Drosophila*. *Nature* **367,** 76–80.

Singh, S., Tang, H. K., Lee, J. Y., and Saunders, G. F. (1998). Truncation mutations in the transactivation region of PAX6 result in dominant-negative mutants. *J. Biol. Chem.* **273,** 21531–21541.

Skeath, J. B., and Doe, C. Q. (1998). Sanpodo and Notch act in opposition to Numb to distinguish sibling neuron fates in the *Drosophila* CNS. *Development* **125,** 1857–1865.

Smoller, D., Friedel, C., Schmid, A., Bettler, D., Lam, L., and Yedvobnick, B. (1990). The *Drosophila* neurogenic locus *mastermind* encodes a nuclear protein unusually rich in amino acid homopolymers. *Genes Dev.* **4,** 1688–1700.

Stoffers, D. A., Stanojevic, V., and Habener, J. F. (1998). Insulin promoter factor-1 gene mutation linked to early-onset type 2 diabetes mellitus directs expression of a dominant negative isoprotein. *J. Clin. Invest.* **102,** 232–241.

Sun, X., and Artavanis-Tsakonas, S. (1997). Secreted forms of DELTA and SERRATE define antagonists of Notch signaling in *Drosophila*. *Development* **124,** 3439–3448.

van de Wetering, M., Cavallo, R., Dooijes, D., van Beest, M., van Es, J., Loureiro, J., Ypma, A., Hursh, D., Jones, T., Bejsovec, A., Peifer, M., Mortin, M., and Clevers. H. (1997). Armadillo coactivates transcription driven by the product of the *Drosophila* segment polarity gene *dTCF*. *Cell* **88,** 789–799.

Verheyen, E. M., Purcell, K. J., Fortini, M. E., and Artavanis-Tsakonas, S. (1996). Analysis of dominant enhancers and suppressors of activated Notch in *Drosophila*. *Genetics* **144,** 1127–1141.

Weinmaster, G. (1997). The ins and outs of Notch signaling. *Mol. Cell. Neurosci.* **9,** 91–102

Xu, T., and Artavanis Tsakonas, S. (1990). *deltex*, a locus interacting with the neurogenic genes *Notch*, *Delta* and *mastermind* in *Drosophila melanogaster*. *Genetics* **126,** 665–677.

Xu, T., Rebay, I., Fleming, R. J., Scottgale, T. N., and Artavanis-Tsakonas, S. (1990). The *Notch* locus and the genetic circuitry involved in early neurogenesis. *Genes Dev.* **4,** 464–475.

Xu, T., and Rubin, G. M. (1993). Analysis of genetic mosaics in developing and adult *Drosophila* tissues. *Development* **117,** 1223–1237.

Yedvobnick, B., Smoller, D., Young, P., and Mills, D. (1988). Molecular analysis of the neurogenic locus *mastermind* of *Drosophila melanogaster*. *Genetics* **118,** 483–497.

Zipursky, S. L., Venkatesh, T. R., Teplow, D. B., and Benzer, S. (1984). Neuronal development in the *Drosophila* retina: Monoclonal antibodies as molecular probes. *Cell* **36,** 15–26.

Received for publication June 16, 1999
Revised August 30, 1999
Accepted August 30, 1999